Power Active Filter Control Based on a Resonant Disturbance Observer

G.A. Ramos Fuentes[1], J.A. Cortés-Romero[1], ZhiXiang Zou[2], R. Costa-Castelló[3], K. Zhou[4]

Abstract

Active filters are power electronics devices used to eliminate harmonics from the distribution network. This article presents an active disturbance rejection control scheme for active filters. The controller is based on a linear disturbance observer combined with a disturbance rejection scheme. The parameter tuning is based on a combined pole placement and an optimal estimation based on Kalman-Bucy filter. Proposed scheme is validated through simulation and experimental work in an active filter.

This paper is a postprint of a paper submitted to and accepted for publication in IET Power Electronics (ISSN 1755-4535) and is subject to Institution of Engineering and Technology Copyright. The copy of record is available at IET Digital Library

I. INTRODUCTION

Shunt active power filters are power electronics devices aimed at preserving the quality of service of the electrical distribution network [1], [2], [3], [4]. They are connected in parallel with nonlinear and reactive loads to compensate the current waveform distortion and phase shift caused by these loads. The control of shunt active power filters is an active research area and several approaches have been proposed in the literature [5], [6], [7], [8], [9]. Most of these strategies are based on two hierarchical control loops: an inner one in charge of assuring the desired network current shape, and an outer one in charge of determining the appropriate power balance. The outer loop displays a slow dynamics and it is usually controlled by means of a Proportional Integral (PI) controller [4].

Although simple controllers, like PI controllers, have been proposed for the current control loop (inner loop), this type of controllers are not usually enough [10], [11], [12] when high performance is required. Usually load currents contain an important number of harmonics, to track/reject this type of signals a high gain at those frequencies is required; this is very difficult to achieve with regular PI controllers. Among others, Internal Model Principle [13] based control techniques offer a good solution to this problem. Repetitive Control (RC) [4] and resonant control [14], [15] are the most popular ones. RC is usually applied using the plug-in architecture. In this architecture the closed-loop poles can be divided in two sets. The closed-loop poles without the repetitive controller and the closed-loop poles of the Repetitive controller which are approximately placed in a circle [16]. This architecture contains only one tuning parameter, $k_r \in (-1, 1)$, which allows to define the radius of the circle which contains the poles. As a consequence the time response has a very limited range of possibilities. In RC different possibilities exist, most relevant ones are AFC [14] and passivity [17], [18] based. In both cases, the stability is not completely guaranteed by construction and complementary elements must be checked or included. Although the time response can be analyzed [19], it is not clear how to design it. In both cases, Repetitive and Resonant control an input-output formulation is used, no disturbance estimation is directly obtained, no signal/noise relationship is analyzed and only limited time response design is possible.

[1]Departamento de Ingeniería Eléctrica y Electrónica, Universidad Nacional de Colombia. garamosf@unal.edu.co, jacortesr@unal.edu.co

[2]School of Electrical Engineering, Southeast University, China. 13913011921@163.com

[3]Universitat Politècnica de Catalunya (UPC) ramon.costa@upc.edu

[4]University of Canterbury (UC) keliang.zhou@canterbury.ac.nz

This work has been partially funded by the following project: MICINN DPI2011-25649 (financed by the Spanish Ministry of Science and Innovation and EU-ERDF funds).

In this paper a disturbance observer based controller is proposed for the inner control loop (current loop). In this way, an active disturbance rejection approach by means of disturbance estimation is proposed for the current control loop of the active filter. Disturbance estimation approach has been previously used with other types of disturbances, one of the first references in this field is the *Disturbance Accommodation Control* (DAC) technique [20], [21]. A closely related trend is the *Active Disturbance Rejection Control* (ADRC) [22] whose main idea is the observer-based disturbance estimation. Gao and his collaborators [23], [24] proposed this paradigm based on partial/total active disturbance rejection.

Recently, following this field, a Generalised Proportional Integral (GPI) observers were introduced in [25] in the context of sliding mode observers for flexible robotics systems. A non-sliding version applied to chaotic systems synchronisation has also been proposed [26]. Linear observers, both for the state and the disturbances have recently been proposed for systems tending to a constant value in steady-state [27].

In this work, the observer is reformulated to incorporate a T_p-periodic disturbance internal model and yields an extended disturbance model with the ability to simultaneously estimate both the states and the disturbance. Differently from other control approaches, this disturbance estimation allows to analyze the load characteristic in real-time.

Simulations and experimental results show that the proposed approach offers similar steady-state performance to those obtained with RC [28] or resonant based control [15]. Moreover proposed scheme constitutes a complete control scheme based on state-space formulation which which guarantees closed-loop stability by construction. Differently from RC and Resonant control, proposed architecture offers a decoupled design for the reference tracking and disturbance rejection problems. Several tuning methodologies are possible, pole placement and optimal control between other. In this work a combined methodology is proposed; pole placement is used for the reference tracking problem while an optimal approach is selected for the disturbance estimation problem.

The paper is organised as follows, section II describes the proposed controller architecture, section III describes the application of proposed controller to the current control in an active filter, section IV describes the experimental platform and shows some experimental results, and finally section V introduces some conclusions and future work.

II. Resonant observer-based control structure

The controller structure in this work is based on an observer scheme which is able to estimate periodic disturbances present in the system. By using the model of the disturbance, an extended plant system is constructed from which the observer is designed. In this way, the observer estimates both the plant system state and the periodic disturbance. This structure is similar to the ADRC case but in this paper a different model of the disturbance is used in order to address the periodic disturbance problem. The disturbance estimation is then added to the control action to reject the actual system disturbance. The problem of having the disturbance entering the system in other channels different from the input channel is also analysed.

Consider the following state-space linear plant model:

$$\dot{\mathbf{x}}_p = \mathbf{A}_p\mathbf{x}_p + \mathbf{B}_p u + \mathbf{B}_p\xi_p \tag{1}$$

$$y = \mathbf{C}_p\mathbf{x}_p \tag{2}$$

where $\mathbf{x}_p \in \mathbb{R}^n$ is the state vector, $u \in \mathbb{R}$ is the control action, $\xi_p \in \mathbb{R}$ is the disturbance signal and $y \in \mathbb{R}$ is the system output. Similarly, $\mathbf{A}_p \in \mathbb{R}^{n\times n}$ is the state transition matrix, $\mathbf{B}_p \in \mathbb{R}^{n\times 1}$ is the input vector and $\mathbf{C}_p \in \mathbb{R}^{1\times n}$ is the output vector. The system defined by $(\mathbf{A}_p, \mathbf{B}_p, \mathbf{C}_p, \mathbf{0})$ is assumed a minimal representation being both controllable and observable. The plant system is assumed to be known and the disturbance ξ_p is T_p-periodic bounded but unknown. It is important to note that in equations (1) and (2) the disturbance ξ_p is added to the input signal u.

A. Disturbance model

Since the disturbance is a T_p-periodic signal it can be approximated by the addition of sinusoidal components

$$\xi = \xi_1 + \xi_2 + \cdots + \xi_m \tag{3}$$

where

$$\xi_k = g_k \sin\left(\omega_k t + \phi_k\right) \tag{4}$$

with g_k the amplitude, ϕ_k the phase and ω_k the frequency. The components can be selected according to the disturbance harmonic content, e. g. in case of full-harmonic content $\omega_k = \frac{2\pi}{T_p}k$, being $k = 0, \ldots, m$.

Each sinusoidal term can be thought as generated by the following linear system, with appropriate initial conditions:

$$\ddot{\xi}_k = -\omega_k^2 \xi_k, \tag{5}$$

which in state space takes the form:

$$\begin{aligned} \dot{\mathbf{z}}_k &= \mathbf{A}_k \mathbf{z}_k \\ \xi_k &= \mathbf{C}_k \mathbf{z}_k \end{aligned}$$

with $\mathbf{z}_k = \left[\xi_k, \dot{\xi}_k\right]^T$, $\mathbf{A}_k = \begin{bmatrix} 0 & 1 \\ -\omega_k^2 & 0 \end{bmatrix}$ and $\mathbf{C}_k = [1, 0]$.

Therefore, the disturbance signal, ξ, admits the following state-space representation:

$$\dot{\mathbf{z}} = \mathbf{A}_\xi \mathbf{z} \tag{6}$$

$$\xi = \mathbf{C}_z \mathbf{z} \tag{7}$$

where $\mathbf{z} = \begin{bmatrix} \mathbf{z}_1^T & \mathbf{z}_2^T & \cdots & \mathbf{z}_m^T \end{bmatrix}^T \in \mathbb{R}^{2m}$ and

$$\begin{aligned} \mathbf{A}_z &= \begin{bmatrix} \mathbf{A}_1 & \mathbf{0} & \mathbf{0} & \cdots & \mathbf{0} \\ \mathbf{0} & \mathbf{A}_2 & \mathbf{0} & \cdots & \mathbf{0} \\ \mathbf{0} & \mathbf{0} & \mathbf{A}_3 & \cdots & \mathbf{0} \\ \vdots & \vdots & \vdots & \ddots & \vdots \\ \mathbf{0} & \mathbf{0} & \mathbf{0} & \cdots & \mathbf{A}_m \end{bmatrix} \\ \mathbf{C}_z &= \begin{bmatrix} \mathbf{C}_1 & \mathbf{C}_2 & \mathbf{C}_3 & \cdots & \mathbf{C}_m \end{bmatrix}. \end{aligned}$$

This internal model has been constructed from a generic T_p-periodic signal with up to m-harmonics. In case that the harmonic content is not exactly known, taking m as an upper bound of the maximum harmonic component would be enough.

In case that the disturbance contains other harmonic distribution, this internal model should be modified accordingly, in power electronic systems there exists systems with only odd-harmonic components [29] or systems with only $6l \pm 1$ harmonic components [30] exists. In case of systems with only odd-harmonic disturbances, matrices A_z and C_z would take the form:

$$\begin{aligned} \mathbf{A}_z &= \begin{bmatrix} \mathbf{A}_1 & \mathbf{0} & \mathbf{0} & \cdots & \mathbf{0} \\ \mathbf{0} & \mathbf{A}_3 & \mathbf{0} & \cdots & \mathbf{0} \\ \mathbf{0} & \mathbf{0} & \mathbf{A}_5 & \cdots & \mathbf{0} \\ \vdots & \vdots & \vdots & \ddots & \vdots \\ \mathbf{0} & \mathbf{0} & \mathbf{0} & \cdots & \mathbf{A}_m \end{bmatrix} \\ \mathbf{C}_z &= \begin{bmatrix} \mathbf{C}_1 & \mathbf{C}_3 & \mathbf{C}_5 & \cdots & \mathbf{C}_m \end{bmatrix}. \end{aligned}$$

Taking advantage of the concrete disturbance particularities in order to reduce the controller complexity reduces the generic controller capabilities (it will not be able to reject those components which have not been considered).

This type of internal model can also be extended to signals composed by multiple frequencies which are not harmonic.

B. Augmented system

We can extend the plant model to include the disturbance signal using $\mathbf{x} = \begin{bmatrix} \mathbf{x}_p^T & \mathbf{z}^T \end{bmatrix}^T \in \mathbb{R}^{n+2m}$, thus we obtain the following augmented model:

$$\dot{\mathbf{x}} = \mathbf{A}\mathbf{x} + \mathbf{B}u \tag{8}$$
$$y = \mathbf{C}\mathbf{x} \tag{9}$$

where:

$$\mathbf{A} = \begin{bmatrix} \mathbf{A}_p & \mathbf{B}_p\mathbf{C}_z \\ \mathbf{0} & \mathbf{A}_z \end{bmatrix}$$
$$\mathbf{B} = \begin{bmatrix} \mathbf{B}_p \\ \mathbf{0} \end{bmatrix}$$
$$\mathbf{C} = \begin{bmatrix} \mathbf{C_p} & \mathbf{0} \end{bmatrix}.$$

This system, with appropriate initial conditions is equivalent to (1)-(2) subject to (3) and (4). It is important to notice that (8)-(9) has no disturbance input and it is an observable system but it is not completely controllable system. The controllable subsystem corresponds to the plant while the non controllable subsystem corresponds to the disturbance model. Note that the disturbance is an exogenous signal consequently it can not be modified through the control action.

C. Resonant observer

In order to observe the state of (8)-(9) a Luenberger observer is proposed:

$$\dot{\hat{\mathbf{x}}} = \mathbf{A}\hat{\mathbf{x}} + \mathbf{B}u + \mathbf{L}\left[y - \mathbf{C}\hat{\mathbf{x}}\right] \tag{10}$$

where $\hat{\mathbf{x}} = \begin{bmatrix} \hat{\mathbf{x}}_p^T & \hat{\mathbf{z}}^T \end{bmatrix}^T$ is the augmented system state estimation and $\mathbf{L} = \begin{bmatrix} \mathbf{L}_p^T & \mathbf{L}_z^T \end{bmatrix}^T$ are the observer gains.

Observer (10) can also be seen as the following closed-loop system:

$$\dot{\hat{\mathbf{x}}} = \left(\mathbf{A} - \mathbf{L}\mathbf{C}\right)\hat{\mathbf{x}} + \mathbf{B}u + \mathbf{L}y. \tag{11}$$

It is important to emphasize that $\hat{\mathbf{z}}$ is composed by $\left[\hat{\mathbf{z}}_1^T, \cdots, \hat{\mathbf{z}}_k^T, \cdots, \hat{\mathbf{z}}_m^T\right]^T$ and the first element of $\hat{\mathbf{z}}_k$, corresponds to the estimation of ξ_k. Therefore, the disturbance estimation is:

$$\hat{\xi} = \mathbf{C}_z\hat{\mathbf{z}}. \tag{12}$$

Defining $\mathbf{e} = \mathbf{x} - \hat{\mathbf{x}} = \left[\mathbf{e}_p^T, \mathbf{e}_z^T\right]^T$ and subtracting the observer system (11) from the system model (8) it is obtained:

$$\dot{\mathbf{e}} = \left(\mathbf{A} - \mathbf{L}\mathbf{C}\right)\mathbf{e}$$

which describes the estimation error dynamics. The characteristic polynomial is defined as:

$$\det\left(s\mathbf{I} - \mathbf{A} + \mathbf{L}\mathbf{C}\right). \tag{13}$$

By means of the gain vector $\mathbf{L}$ the eigenvalues of the observer can be placed as desired.

D. Equivalent input disturbance estimation

The previous sections where devoted to estimate a disturbance that is added to the input of the system. In this section, we are going to show that, under some assumptions, the same strategy can be used to reject disturbances that enter the system at different channels; this can be done using the equivalent input disturbance concept [31].

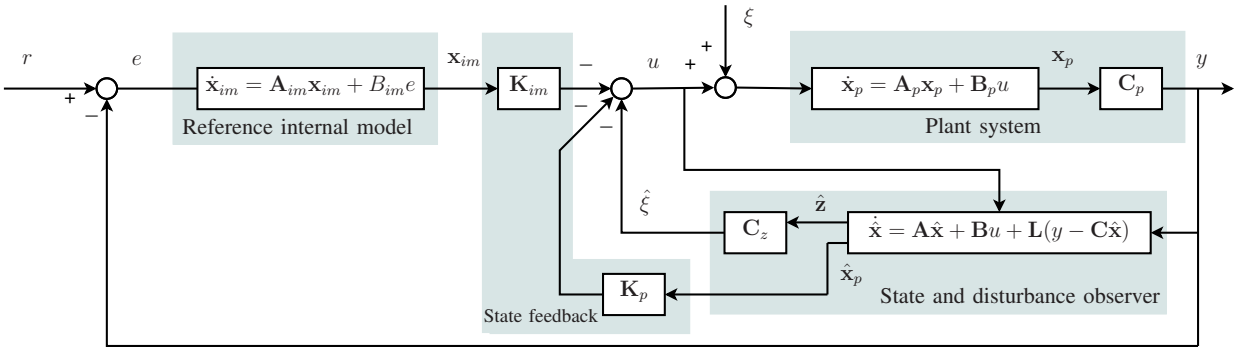

Figure 1. Proposed controller architecture. The controller is composed by an observer, a disturbance estimation/cancellation, a state feedback and a reference internal model.

1) State disturbance: Consider the following model where the disturbance uses a different channel form the input to enter the system state:

$$\dot{\mathbf{x}}_s = \mathbf{A}_p\mathbf{x}_s + \mathbf{B}_p u + \mathbf{B}_s\xi_s \tag{14}$$

$$y_s(t) = \mathbf{C}_p\mathbf{x}_s, \tag{15}$$

with ξ_s being a state disturbance and $\mathbf{B}_s \in \mathbb{R}^{n\times 1}$ the disturbance input vector. We want to establish a equivalence between system (1)-(2) and system (14)-(15). To accomplish this it is necessary that:

$$\mathbf{B}_s\xi_s = \mathbf{B}_p\xi_p. \tag{16}$$

In this way, by means of least square approach we find that:

$$\xi_p = \left(\mathbf{B}_p^T\mathbf{B}_p\right)^{-1}\mathbf{B}_p^T\mathbf{B}_s\xi_s, \tag{17}$$

where ξ_p is called the equivalent input disturbance regarding system (14)-(15). Thus, applying the observer scheme in previous section, II-C, to system (14)-(15) we are estimating the equivalent input disturbance ξ_p that can be added to the control signal to reject the disturbance ξ_s.

In Single Input Single Output (SISO) systems $\mathbf{B}_p^T\mathbf{B}_p$ is a scalar number different from zero, consequently $\left(\mathbf{B}_p^T\mathbf{B}_p\right)^{-1}$ always exist.

2) Output disturbance: Now we can consider a system in which there's also a disturbance at the output, ξ_o:

$$\dot{\mathbf{x}}_o = \mathbf{A}_p\mathbf{x}_o + \mathbf{B}_p u + \mathbf{B}_p\xi_s \tag{18}$$

$$y_o = \mathbf{C}_p\mathbf{x}_o + \xi_o, \tag{19}$$

In this system, it is said that there exists an equivalence between an input disturbance ξ_s and the output disturbance, if given a bounded ξ_o there exist a bounded ξ_s and appropriate initial conditions that produce the same output, y_o. Therefore, if this condition holds, for the output disturbance case we can always apply the disturbance observer proposed in Section II-C to reject such disturbance.

3) Disturbance compensation in steady-state: In subsection II-D2 and II-D1 it has been shown that under certain circumstances it is possible to instantaneously compensate the disturbance, for those cases in which this is not possible, it is always possible to asymptotically cancel the disturbance effect over the output. That is, given a system like (18)-(19), where ξ_o is a T_p-periodic signal coming from an output disturbance or being the steady-state effect of a T_p-periodic state disturbance, if $(A_p, B_p, C_p, 0)$ is a controllable system with no zeros at frequencies ω_k, it is always possible to obtain a bounded T_p-periodic signal, u, which makes $y_o = 0$ in steady state. As a consequence, if instantaneous cancellation is not possible it will be possible the asymptotic cancellation.

Although the instantaneous cancellation is possible, proposed disturbance observer has an exponential convergence, as a consequence the disturbance cancellation will also be exponential.

E. Disturbance rejection using a resonant observer

Figure 1 shows the general structure for a servo system with the proposed active disturbance rejection strategy. In this structure an internal model has been added with the aim of providing reference tracking properties to the system:

$$\dot{\mathbf{x}}_{im} = \mathbf{A}_{im}\mathbf{x}_{im} + \mathbf{B}_{im}\left(r - y\right). \tag{20}$$

Remark 1: In case of requiring asymptotic tracking for a single sinusoidal signal with frequency ω_1 we should add a resonant element as internal model, as consequence $\mathbf{A}_{im} = \begin{bmatrix} 0 & 1 \\ -\omega_1^2 & 0 \end{bmatrix}$ and $\mathbf{B}_{im} = [0, 1]^T$.

In this manner, a state-feedback controller for the plant state system (1)-(2) could be applied using the state estimation obtained through the observer (11):

$$u = \mathbf{K}_{im}\mathbf{x}_{im} - \mathbf{K}_p\hat{\mathbf{x}}_p - \mathbf{C}_z\hat{\mathbf{z}}. \tag{21}$$

where $\mathbf{K}_{im}$ and $\mathbf{K}_p$ are the internal model and state feedback gains respectively. The control law seeks for disturbance rejection by means of the term $\mathbf{C}_z\hat{\mathbf{z}}$, see (12).

With this controller the following state transition matrix of the overall closed-loop system is obtained:

$$\begin{bmatrix} \mathbf{A}_a - \mathbf{B}_a\mathbf{K}_a & -\mathbf{B}_a\mathbf{K} \\ \mathbf{0} & \mathbf{A} - \mathbf{L}\mathbf{C} \end{bmatrix} \tag{22}$$

with $\left[\mathbf{x}_p{}^T, \mathbf{x}_m^T, \mathbf{e}_p^T, \mathbf{e}_z{}^T\right]^T$ as state vector and

$$\begin{aligned} \mathbf{A}_a &= \begin{bmatrix} \mathbf{A}_p & \mathbf{0} \\ -\mathbf{B}_{im}\mathbf{C}_p & \mathbf{A}_{im} \end{bmatrix} \\ \mathbf{B}_a &= \begin{bmatrix} \mathbf{B}_p \\ \mathbf{0} \end{bmatrix} \\ \mathbf{K}_a &= [\mathbf{K}_p \; -\mathbf{K}_{im}] \\ \mathbf{K} &= [\mathbf{K}_p \, \mathbf{C}_z]. \end{aligned}$$

The closed-loop dynamics can be determined by fixing the eigenvalues of transition matrix (22). This can be done through $\mathbf{K}_p$, $\mathbf{K}_{im}$, $\mathbf{L}_p$ and $\mathbf{L}_z$. From (22) and based on the separation principle [32] the control vector gains $\mathbf{K}_p$ and $\mathbf{K}_{im}$ can be designed independently of the estimation gains $\mathbf{L}_p$ and $\mathbf{L}_z$.

F. Controller tuning

Proposed method architecture includes, both the reference and the disturbance internal models. Applying the Internal Model Principle, this guarantees steady-state null error if the system is stable. As a consequence, steady-state performance obtained will be similar to the one obtained using a Repetitive Control or Resonant Control. In comparison to these methods proposed architecture can guarantee closed-loop stability by construction; the architecture has $\mathbf{K}_a$ and $\mathbf{L}$ as design parameters. These parameters could be fixed in different ways:

- Placing closed-loop poles. By fixing the poles of (22) most relevant components of the time response can be completely specified (i.e. convergence time and oscillation frequency between others).
- Optimal design. The solution of many relevant control/estimation problems [33] can be formulated as a state feedback or combined observer plus state feedback, consequently $\mathbf{K}_a$ and $\mathbf{L}$ can be designed according to these problems[33].
- Combined methods. Taking profit from the structure of (22) it is possible to design the parameters in a decoupled manner. This allows to differently treat the reference tracking and the disturbance rejection.

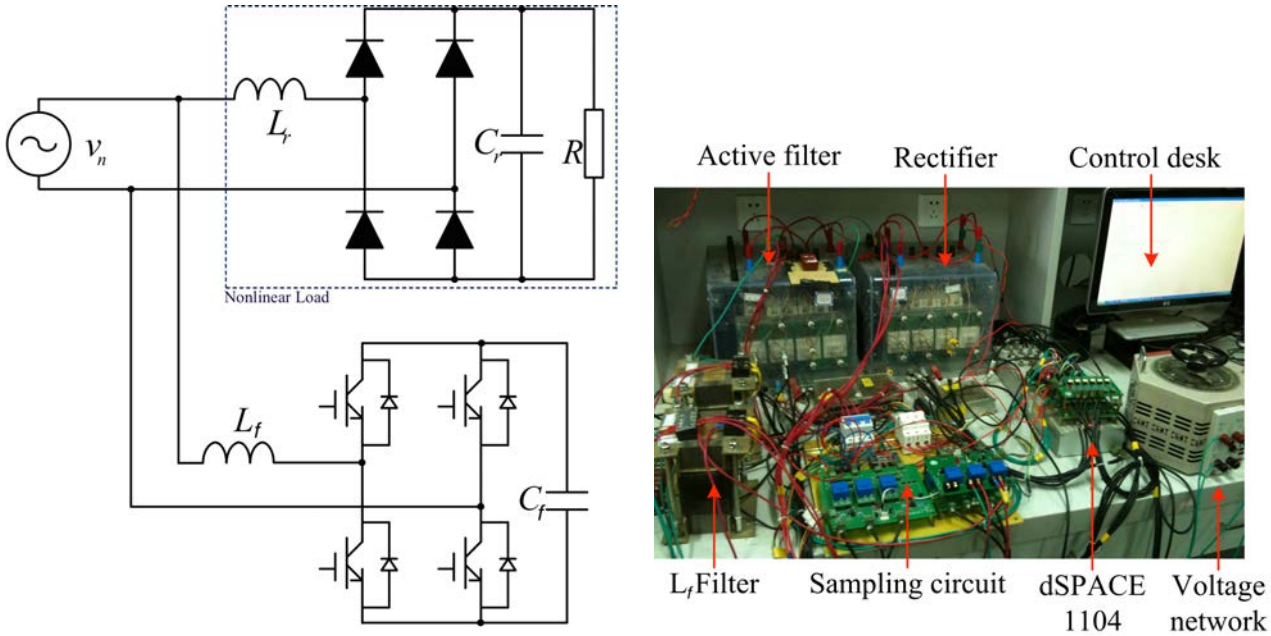

(a) (b)

Figure 2. Single-phase shunt active filter connected to the network-load system (full bridge-rectifier with a resistive load) : (a) Schematics, (b) Experimental setup view.

In this work the third option will be applied. In the proposed architecture it is important that the current controller follows the current reference rapidly, this simplifies the outer control loop (i.e. the voltage control loop). These type of specification can be easily accomplished by placing the poles of $\mathbf{A}_a - \mathbf{B}_a\mathbf{K}_a$ through the values of $\mathbf{K}_p$ and $\mathbf{K}_{im}$.

The disturbance rejection proposed scheme is based on an explicit disturbance estimation and cancellation. In this context is it convenient to estimated in an optimal manner. It is well-known that the Kalman-Bucy filter constitutes the optimal Luenberger observer where the estimation error covariance is minimized [33]. The optimal observer gain is defined by:

$$\mathbf{L} = \mathbf{P}\mathbf{C}^T\mathbf{V}^{-1}$$

where $\mathbf{P}$ is the unique positive-semidefinite solution of the algebraic Riccati equation:

$$\mathbf{P}\mathbf{A}^T + \mathbf{A}\mathbf{P} - \mathbf{P}\mathbf{C}^T\mathbf{V}^{-1}\mathbf{C}\mathbf{P} + \mathbf{W} = \mathbf{0},$$

being $\mathbf{V}$ and $\mathbf{W}$ the spectral density matrices of the measurement and process noise respectively.

G. Implementation issues

According to previous developments the controller to be implemented is defined by the following dynamical system:

$$\dot{\mathbf{x}}_{im} = \mathbf{A}_{im}\mathbf{x}_{im} + \mathbf{B}_{im}\left(i_d - i_n\right) \quad (23)$$

$$\dot{\hat{\mathbf{z}}} = \mathbf{A}_z\hat{\mathbf{z}} + \mathbf{L}_z\left(i_n - \mathbf{C}_p\hat{\mathbf{x}}_p\right) \quad (24)$$

$$\dot{\hat{\mathbf{x}}}_p = \left(\mathbf{A}_p - \mathbf{L}_p\mathbf{C}_p\right)\hat{\mathbf{x}}_p + \mathbf{B}_p\mathbf{C}_z\hat{\mathbf{z}} + \mathbf{B}_p u + \mathbf{L}_p i_n \quad (25)$$

$$u = \mathbf{K}_{im}\mathbf{x}_{im} - \mathbf{K}_p\hat{\mathbf{x}}_p - \mathbf{C}_z\hat{\mathbf{z}}. \quad (26)$$

As shown in section II-A, $\mathbf{A}_z$ is not a dense matrix, it is plenty of 0s. Consequently, it is not convenient to directly implement (24). To reduce the computational burden it is possible to take profit from the structure of (24). The components of $\dot{\hat{\mathbf{z}}}$ can be computed as:

$$\dot{\hat{\mathbf{z}}}_k = \mathbf{A}_k\hat{\mathbf{z}}_k + \mathbf{L}_z^k\left(i_n - \mathbf{C}_p\hat{\mathbf{x}}_p\right) \quad (27)$$

where $\mathbf{L}_z^k$ are the components of $\mathbf{L}_z^T = \left[(\mathbf{L}_z^1)^T, (\mathbf{L}_z^2)^T, \cdots, (\mathbf{L}_z^m)^T\right]$. With this transformation the computational burden of the proposed architecture is quite similar to that of a resonant controller.

III. Active power filter

A. The boost converter

An active filter is an electronic device connected in parallel with nonlinear/reactive loads (see Figure 2.a) which goal is making the network current to be a sinusoidal one in phase with the voltage signal (i.e. to guarantee unity power factor at the network side), $i_n^* = I_d^* \sin(\omega_n t)$[1]. In this work, a boost converter is used as active filter.

The averaged (at the switching frequency) and linearized model of the boost converter is given by

$$L_f \frac{di_f}{dt} = -r_L i_f + v_n - V_{dc} d \tag{28}$$

$$C_f \frac{dV_{dc}}{dt} = i_f d - \frac{V_{dc}}{r_C} \tag{29}$$

with $d \in [-1, 1]$ is the PWM duty ratio, V_{dc} is the dc capacitor voltage, i_f is the inductor current, L_f is the converter inductor, r_L is the inductor parasitic resistance, C_f is the converter capacitor, r_C is the capacitor parasitic resistance and $v_n = V_n\sqrt{2}\sin(\omega_n t)$ is the voltage source[2]. Equations (28)-(29) can be partially linearized with the variable changed $\alpha = V_{dc} d$, $E_C = \frac{1}{2} C_f V_{dc}^2$:

$$L_f \frac{di_f}{dt} = -r_L i_f + v_n - \alpha \tag{30}$$

$$\frac{dE_C}{dt} = -\frac{E_C}{r_C C_f} + i_f \alpha \tag{31}$$

Due to the nature of the voltage source and assumed loads, the steady-state load current is usually a periodic signal with only odd-harmonics in its Fourier series expansion, so it can be written as $i_l = \sum_{k=0}^{\infty} a_k \sin(\omega_n (2k+1) t) + b_k \cos(\omega_n (2k+1) t)$.

Another collateral goal, necessary for a correct operation of the converter, is to assure constant average value of the dc bus voltage[3], i.e. $< V_{dc} >_0^* = v_d$, where v_d must fulfill the boost condition ($v_d > \sqrt{2} v_n$).

The controller follows the two level approach proposed in [28] and portrayed in Fig. 3: first, an inner current controller forces the sine wave shape for the network current and, second, an outer voltage control loop yields the appropriate active power balance for the whole system. The output of this loop is the amplitude of the sinusoidal reference for the current control loop. The active power balance is achieved if the energy stored in the active filter capacitors, E_C, is equal to a reference value, E_C^d [28]. As E_C contains intrinsic oscillations, its mean value $< E_C >_{T_p}$[4] is used to achieve this goal. Usually a PI controller over the energy error ($E_C^d - < E_C >_{T_p}$) has been used [28].

In this work, the following parameters have been used $L_f = 5\text{mH}$, $C_f = 1100\mu F$, $r_L = 0.2\ \Omega$, $r_C = 8200\ \Omega$, $v_n = 90\text{V}$ (peak value), and dc-link voltage $V_{dc} = 250\text{V}$.

In this work, the outer control loop will be composed by a regular PI controller and the current controller will follow the structure introduced in section II and discussed in the following subsection.

[1] x^* represents the steady-state value of signal $x(t)$.

[2] $\omega_n = 2\pi/T_p$ rad/s is the network frequency.

[3] $< x >_0$ means the dc value, or mean value, of the signal $x(t)$.

[4] $< x >_{T_p} = \int_{t-T_p}^{t} x(\tau) d\tau$

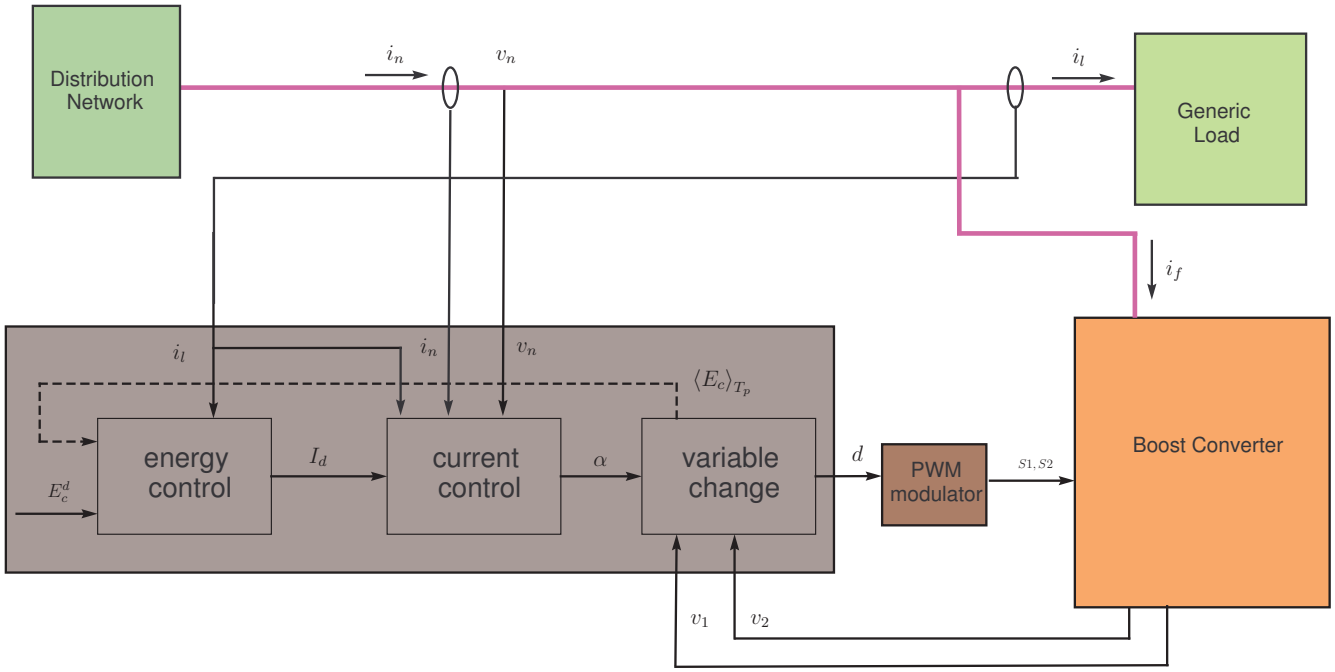

Figure 3. Active filter complete control architecture. The scheme uses a two level approach composed by an inner current control (analyzed in this paper) and an outer voltage controller[28].

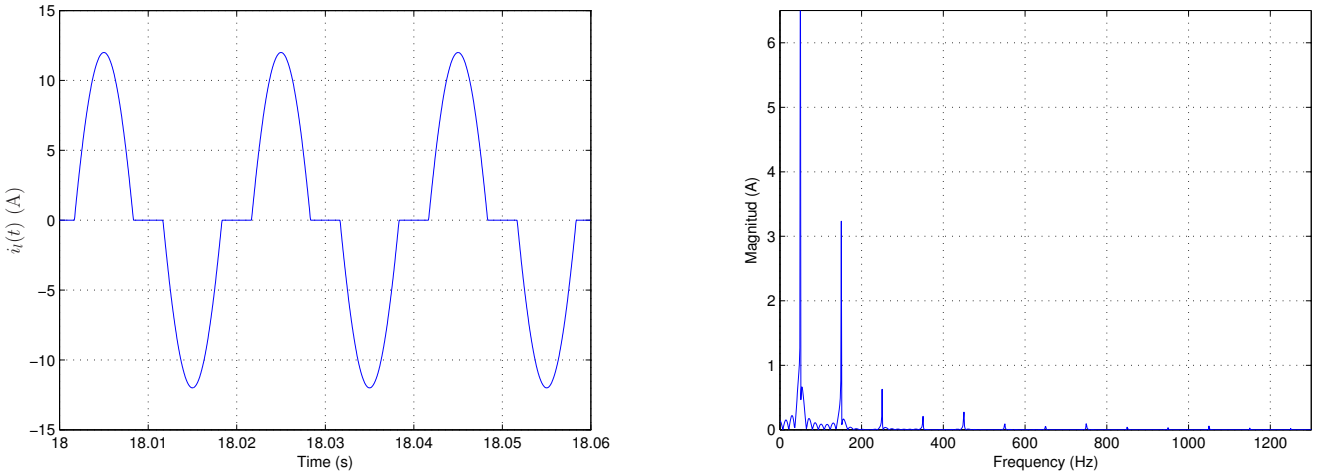

(a) (b)

Figure 4. Full-bridge rectifier with a resistive steady-state load current $i_l(t)$: (a) waveform, (b) harmonic content.

B. Current controller design and simulation results

The plant system is defined by equation (30) and following Figure 2.a. Therefore, since the control objective is to provide a sinusoidal current, $i_n = i_f + i_l$, in phase with the voltage network v_n, we can treat the current i_l as an output disturbance, see Section II-D2. Thus, in this case we are estimating the equivalent input disturbance related to i_l and the reference for this loop is constructed from the output of the outer loop, i.e. $r = I_d \sin(\omega t)$. Figure 5 shows described current control scheme.

Since the reference is a 50 Hz sinusoidal signal a resonant element is used as internal model: $\mathbf{A}_{im} = \begin{bmatrix} 0 & 1 \\ -(2\pi 50)^2 & 0 \end{bmatrix}$ and $\mathbf{B}_{im} = [0, 1]^T$.

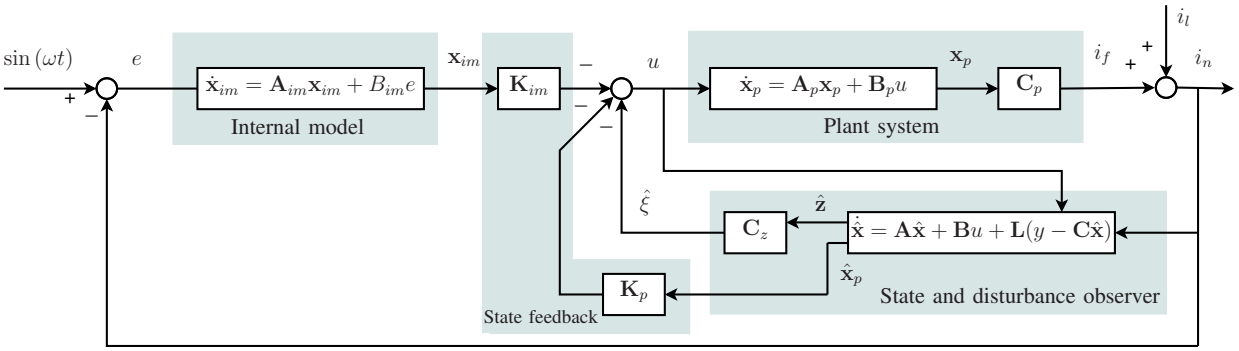

Figure 5. Proposed current controller control scheme. The scheme is composed by a disturbance observer used to cancel de disturbance effect, a state feedback and a reference internal model.

As argued in subsection II-F, the controller tuning will follow a two step approach will be followed. Firstly the reference tracking subsystem is tunned non-oscillatory and faster than the energy loop (see [28] for details) and to allow fast tracking convergence. This is achieved placing the closed-loop poles at $-500\,\mathrm{rad/s}$, accordingly the controller parameters are $\mathbf{K}_p = 37.5$ and $\mathbf{K}_{im} = [-73.35,\ 651.3]$.

The current i_l is simulated to approximate a current produced by a nonlinear load composed of a full bridge diode rectifier with a resistive load. The current i_l has a Total Harmonic Distortion (THD) of $67.43\ \%$, its waveform and its harmonic content are shown in Figures 4.a and 4.b, respectively. As it can be seen in Figure 4.b this current contains harmonics placed only at odd components.

The disturbance observer is constructed including 15 resonant elements in the disturbance estimator. The selected frequencies are the fundamental voltage network frequency of 50 Hz ($\omega_1 = 2\pi 50\ \mathrm{rad/s}$) and the subsequent 14 odd-harmonic frequency components ($\omega_k = 2\pi 50(2k+1)\ \mathrm{rad/s}$ with $k = 1, \cdots, 14$).

In order to obtain the estimator parameters, $V = 1$ and $\mathbf{W} = \gamma\,[0\ \mathbf{Cz}]^T\,[0\ \mathbf{Cz}]$ where $\gamma = 1000$ have been selected. This selection represents a good compromise between system noise and observer bandwidth.

Since the observer goal is estimating the equivalent input disturbance, the original disturbance, the load current in this case, can be obtained through the following filter:

$$\hat{i}_l(s) = \mathbf{C_p}\,(s\mathbf{I} - \mathbf{A_p})^{-1}\,\mathbf{B_p}\hat{\xi}(s). \tag{32}$$

This means that since the disturbance in (1)-(2) is placed at the plant system input while in the active filter it is placed at the output, the equivalent input disturbance estimation $\hat{\xi}$ must be taken to the output through the plant model in order to obtain a estimation of the load current $\hat{i}_l$.

The path from i_l to $\hat{\xi}$ and then to $\hat{i}_l$ is found to be:

$$\frac{\hat{i}_l(s)}{i_l(s)} = \mathbf{C_p}\,(s\mathbf{I} - \mathbf{A_p})^{-1}\,\mathbf{B_p}\mathbf{C}_z\,(s\mathbf{I} - \mathbf{A}_p + \mathbf{LC})^{-1}\,\mathbf{L}. \tag{33}$$

Figure 6.a shows the frequency response of (33). As it can be seen it has a low pass profile but with gain equal to 1 at the frequencies where the disturbance components are assumed to be. This characteristics guarantee that only those frequency components which belong to the assumed disturbance can contribute to the estimation without deformation. Figure 6.b shows $i_l(t)$ and $\hat{i}_l(t)$ in the steady-state. As it can be seen both signals are qualitatively equal, consequently the estimator is working precisely. Figure 6.c shows the steady-state evolution of $\hat{z}_1$, $\hat{z}_3$, $\hat{z}_5$, $\hat{z}_7$ and $\hat{z}_9$ which correspond to the estimation of most relevant frequency components. As it can be seen all of them are sinusoidal signals of the appropriate frequency, from these signals it is possible to extract most relevant information about the load current.

Figure 7.a shows the voltage network $v_n(t)$, the reference current i_d and the network current i_n when the complete control system is applied. As it can be seen, the system successfully tracks the reference signal which is in phase with the voltage network, thus achieving unitary power factor.

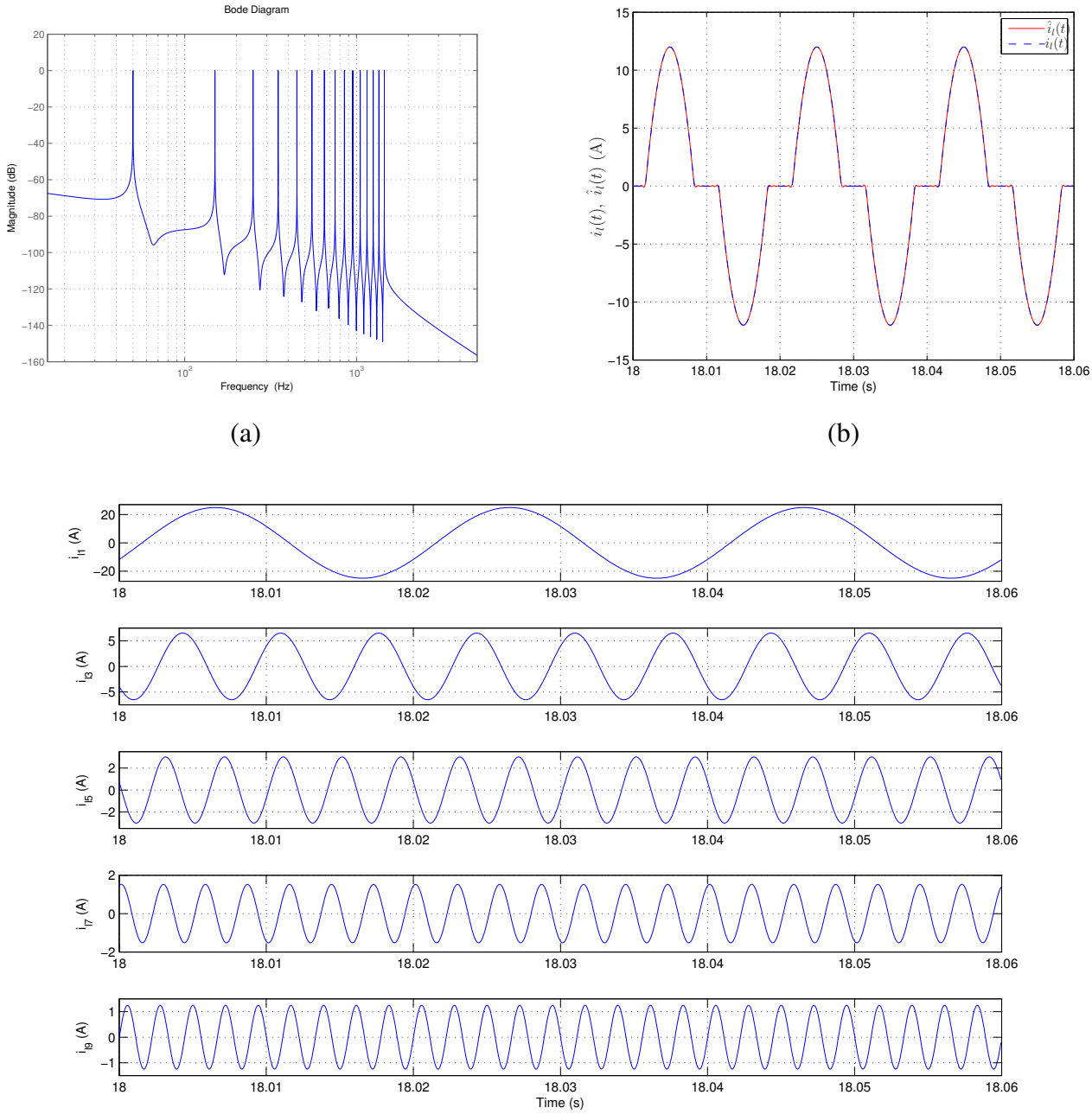

Figure 6. Disturbance observer: (a) Frequency response, (b) Steady-state disturbance estimation through $i_l(t)$ (blue) and $\hat{i}_l(t)$ (green) comparison, (c) Steady-state component estimation for $\hat{i}_l(t)$.

Figure 7.b shows $i_n(t)$ harmonic content. It can be noticed that still small high order frequency components are presented in the current. The harmonic content of $i_n(t)$ which has a THD of $1.217\ \%$. It is shown that frequency components until the 31^{th} are highly reduced, below -50 dB.

This same scenario has been simulated using PI controllers instead of the proposed one. An IMC-based algorithm[34] and the AMIGO [35] have used to tune the controller. In both cases a THD over $10\ \%$ has been obtained. As expected proposed controller offers a better steady-state behavior which justifies the

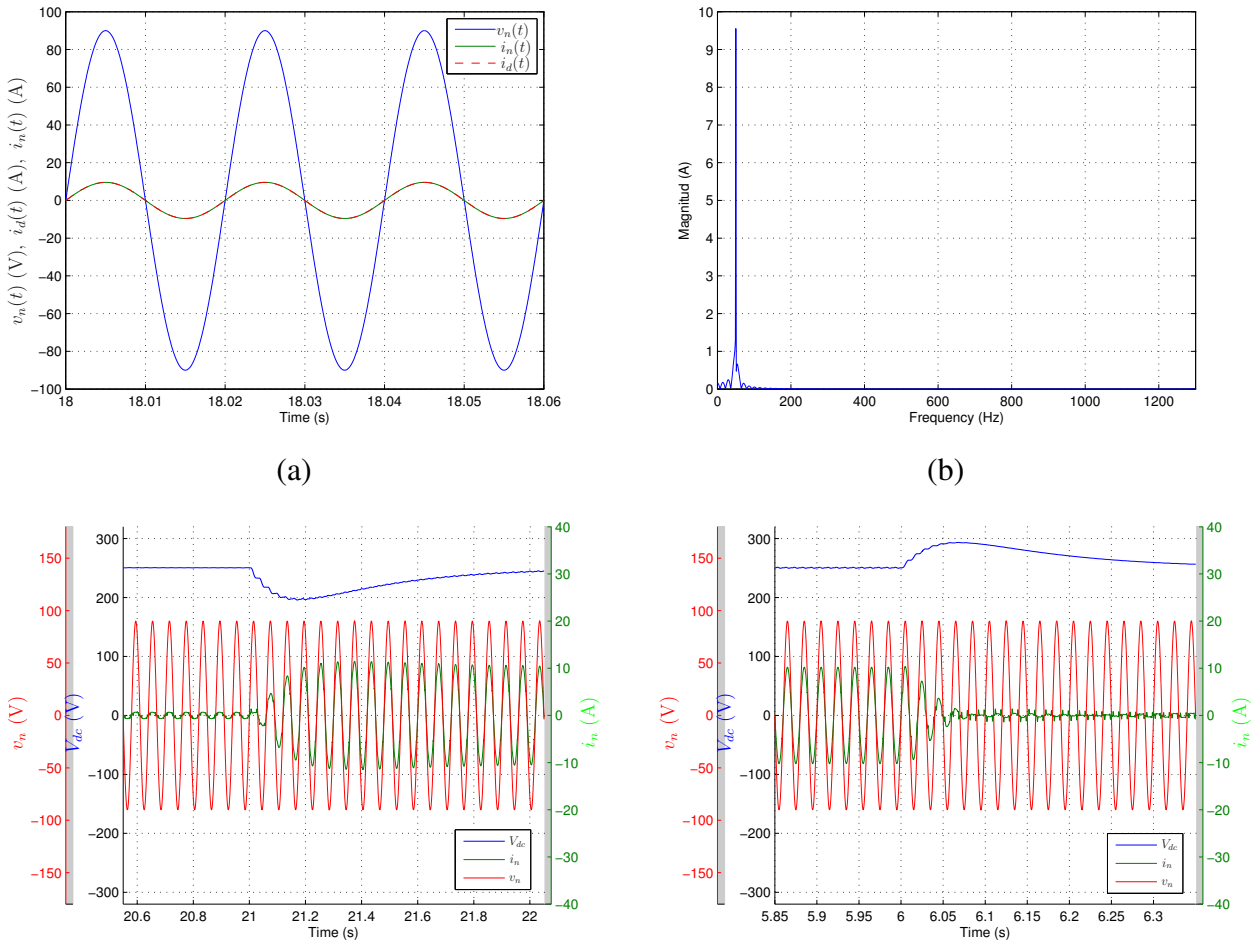

Figure 7. Closed-loop simulaton results. (a) Steady-state network voltage $v_n(t)$ (blue), reference current $i_d(t)$ (green) and network current $i_n(t)$ (red) waveforms. (b) Steady-state network current, $i_n(t)$, harmonic content. (c) and (d) Network voltage, v_n, network current, $i_n(t)$, and DC-link voltage, V_{dc}, waveforms from no-load to full nonlinear load (c) and from full nonlinear load to no-load (d).

controller complexity increase.

Figure 7.c and Figure 7.d, show the evolution of V_{dc}, i_n and v_n when a load is turned on from void (Figure 7.c) and when a load is turned off (Figure 7.d). As it can be seen after a small transient the voltage, V_{dc}, stabilizes at the desired value and i_n follows the desired profile. As expected, V_{dc} contains small amplitude intrinsic oscillations and only its mean value is regulated.

The active filter steady-sate behavior has also been tested with other types of load currents with a very important harmonic content, between others a current profile generated by a single-phase thyristor rectifier bridge (Figure 8) and the parallel connection of the full bridge diode rectifier and the single-phase thyristor rectifier bridge (Figure 9). In all the cases the THD was belong 1.56 % and the Power Factor was higher than 0.9997.

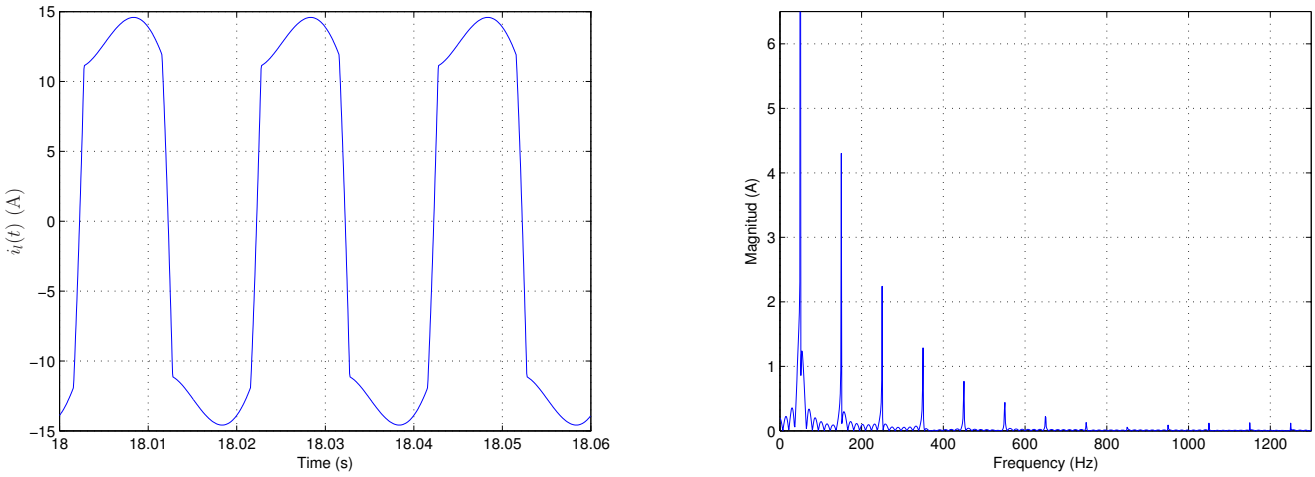

(a) (b)

Figure 8. Thyristor bridge rectifier with a resistive steady-state load current, $i_l(t)$: (a) waveform, (b) harmonic content.

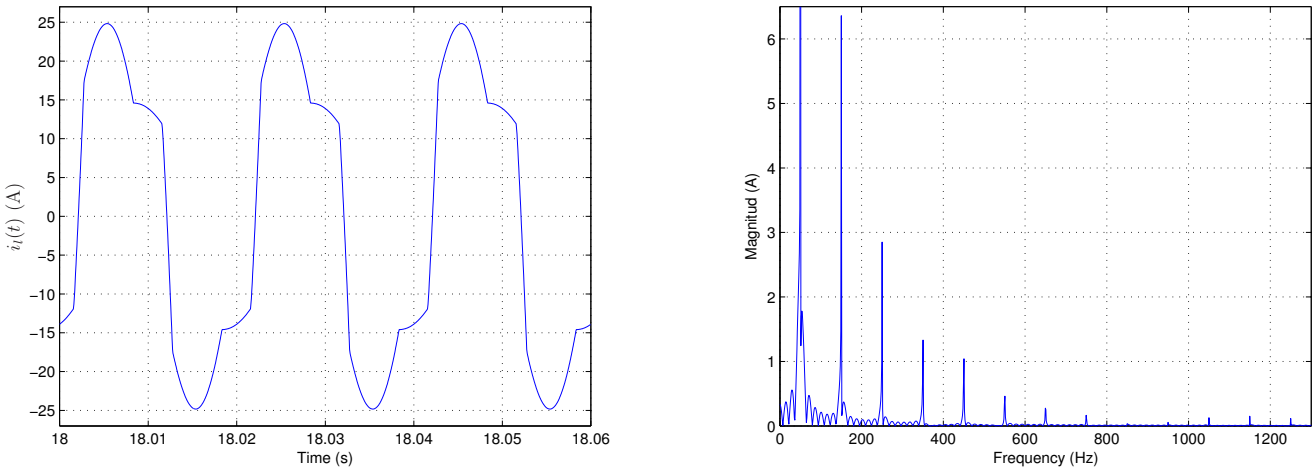

(a) (b)

Figure 9. Thyristor bridge in parallel with a diode full-bridge steady-state load current, $i_l(t)$: (a) waveform, (b) harmonic content.

IV. EXPERIMENTAL RESULTS

To experimentally validate the proposed control strategy an active filter has been built. The laboratory setup is illustrated in Figure 2.b. The experimental prototype (see the schematics in Figure 2.a) is based on a Semikron AN-8005 (an H-bridge IGBT inverter), and the controller has been implemented a dSPACE DS1104 controller card. The experimental setup has the same parameters that have been used in the simulation (section III) and the controller is exactly the same. The converters uses a sampling and switching frequency of $5\,\mathrm{kHz}$. To perform the experiments the voltage is obtained from the grid through a transformer, clearly it is not an ideal voltage because it contains some harmonics (as can be seen in Figure 10.b).

Figure 10.a shows the steady-state network current when the active filter is off and the load current that will be used to perform the experiments. This current corresponds to the one generated by rectifier defined to feed a dc-load composed by a resistance of $R = 18\,\Omega$ (the diode-bridge contains a series inductance of $L_r = 5\,\mathrm{mH}$ on the ac-side, and a capacitor with $C_r = 1100\,\mu F$ in the dc-side). As it can be seen, this current contains an important harmonic content (Figure 10.a) achieving a 31.95% THD. It is important

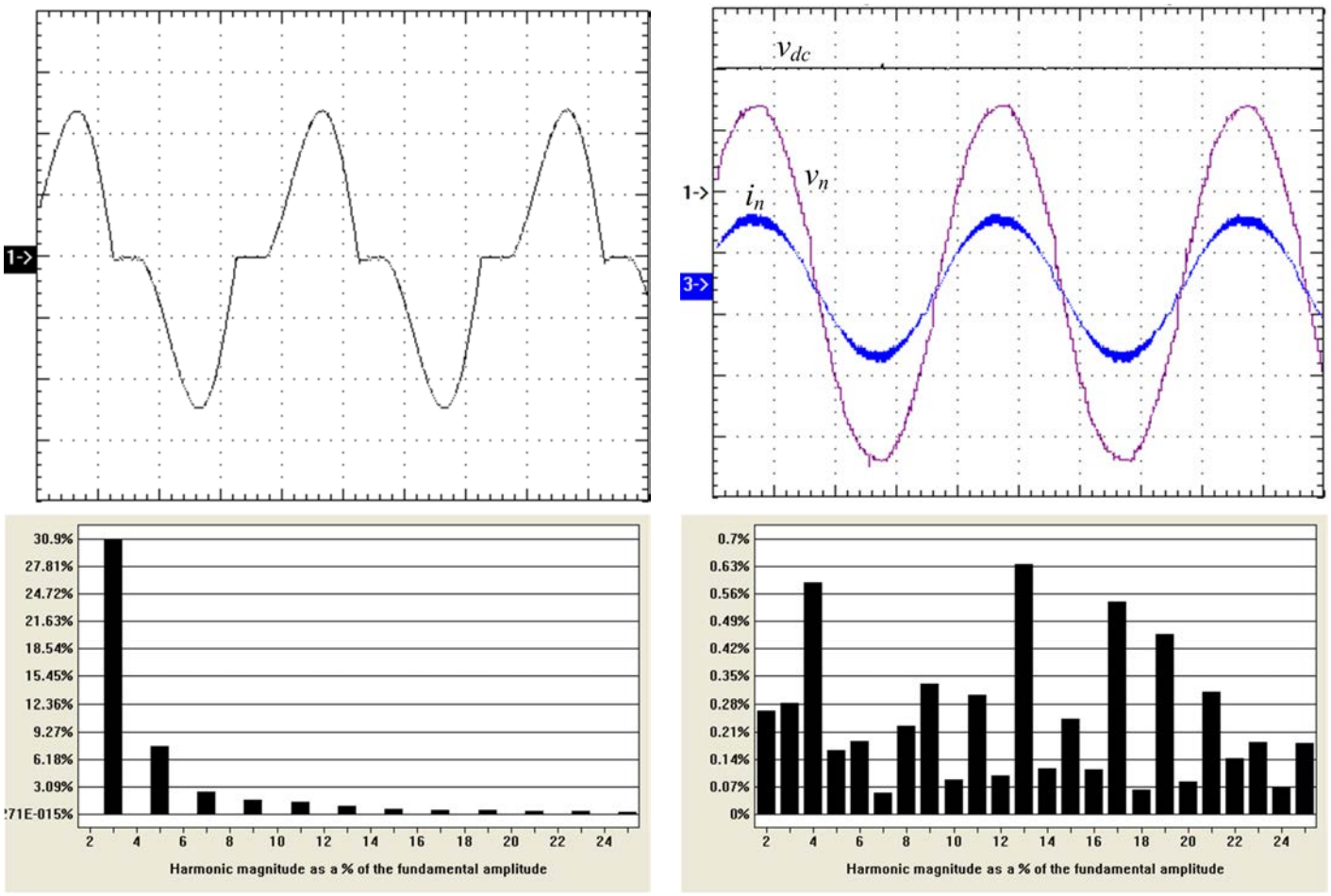

(a) (b)

Figure 10. (a) Load current, i_l, waveform (x: 5ms/div; y: 5A/div) (top) and harmonic content of load current il without active filter ($THD = 31.948\%$) (bottom). (b)Network current, i_n, waveform (x: 5ms/div; y: 10A/div) (top) and harmonic content of network current in with active filter (THD = 1.420%, $\cos\psi = 0.99$) (bottom).

to note that only odd components are present in the harmonic contents.

Figure 10.b shows the steady-state network current when the active current is on and the load is the one described previously. As it can be seen the current is almost a perfect sinusoidal waveform in phase with the voltage waveform. It can be seen that the harmonic content is very small and it has a 1.42% THD and a $\cos\phi = 0.99$. As a consequence, the system is working properly and fulfilling the regulation requirements. It is important to see that inspite this voltage source imperfection the controller provides an excellent performance.

Figure 11 shows the transient evolution of both the dc-bus voltage, V_{dc} and the network current, i_n, when a load is turned on (Figure 11.a) and the load is turned off (Figure 11.b). In both cases, both the voltage and the current reach the steady-state in less than 5 cycles, and they are always bounded. Results are satisfactory and quite similar to the ones obtained in simulation.

V. CONCLUSIONS

In this paper a new approach for the current control design and tuning used in two level active filter control architectures has been presented. Proposed architecture offers excellent steady-state performance (similar to that of repetitive and resonant control) in a simple and formal framework. Different form others other common schemes stability is guaranteed by construction, tuning criteria have also been analyzed and proposed.

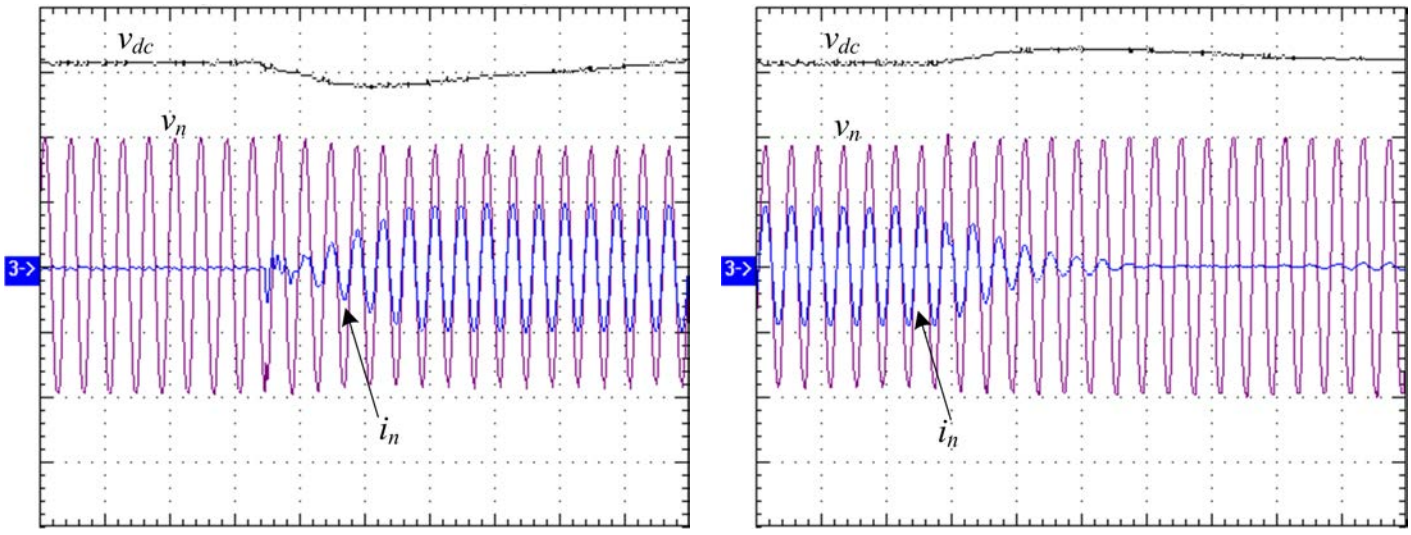

Figure 11. Network voltage, v_n, (purple), network current, i_n, (blue) and DC-link voltage (black) waveforms (x: 50ms/div; y: 45V/div, 10A/div and 80V/div, respectively): from no-load to full nonlinear load (a) and from full nonlinear load to no-load (b).

The architecture is composed by a disturbance observer and a feedback controller. The disturbance observer output is used to cancel the disturbance effect while the feedback controller (composed by and internal model and a state feedback/estimation) is used to impose the desired dynamical behavior and to accomplish the tracking specifications. Both elements fulfill the separation principle so they can be designed and analyzed separately.

Differently to other controllers this architecture allows obtaining information about the disturbance. The disturbance (i.e. load current) frequency components are obtained, consequently load current most relevant information can be easily extracted. This is of special interest in some applications like the active filter .

REFERENCES

[1] H. Akagi, "New trends in active filters for power conditioning," *IEEE Trans. Ind. Applicat.*, vol. 32, no. 6, pp. 1312–1322, Nov. 1996.

[2] A. Varschavsky, J. Dixon, M. Rotella, and L. Moran, "Cascaded nine-level inverter for hybrid-series active power filter, using industrial controller," *IEEE Trans. Ind. Electron.*, vol. 57, no. 8, pp. 2761 –2767, Aug. 2010.

[3] V. Corasaniti, M. Barbieri, P. Arnera, and M. Valla, "Hybrid active filter for reactive and harmonics compensation in a distribution network," *IEEE Trans. Ind. Electron.*, vol. 56, no. 3, pp. 670 –677, Mar. 2009.

[4] R. Griñó, R. Cardoner, R. Costa-Castelló, and E. Fossas, "Digital repetitive control of a three-phase four-wire shunt active filter," *IEEE Transactions on Industrial Electronics*, vol. 54, no. 3, pp. 1495–1503, Jun. 2007.

[5] M. Ketzer and C. Brandao Jacobina, "Multivariable load current sensorless controller for universal active power filter," *Power Electronics, IET*, vol. 7, no. 7, pp. 1777–1786, July 2014.

[6] T. N. Nguyen, A. Luo, Z. Shuai, M. T. Chau, M. Li, and L. Zhou, "Generalised design method for improving control quality of hybrid active power filter with injection circuit," *Power Electronics, IET*, vol. 7, no. 5, pp. 1204–1215, May 2014.

[7] M. Odavic, V. Biagini, P. Zanchetta, M. Sumner, and M. Degano, "One-sample-period-ahead predictive current control for high-performance active shunt power filters," *IET Power Electronics*, vol. 4, pp. 414–423(9), April 2011.

[8] C.-C. Hua, C.-H. Li, and C.-S. Lee, "Control analysis of an active power filter using lyapunov candidate," *IET Power Electronics*, vol. 2, pp. 325–334(9), July 2009.

[9] F. Freijedo, J. Doval-Gandoy, O. Lopez, P. Fernandez-Comesana, and C. Martinez-Penalver, "A signal-processing adaptive algorithm for selective current harmonic cancellation in active power filters," *IEEE Trans. Ind. Electron.*, vol. 56, no. 8, pp. 2829 –2840, 2009.

[10] S. Buso, L. Malesani, and P. Mattavelli, "Comparison of current control techniques for active filters applications," *IEEE Trans. Ind. Electron.*, vol. 45, no. 5, pp. 722–729, 1998.

[11] Q.-N. Trinh and H.-H. Lee, "An advanced current control strategy for three-phase shunt active power filters," *Industrial Electronics, IEEE Transactions on*, vol. 60, no. 12, pp. 5400–5410, Dec 2013.

[12] Z. Shuai, A. Luo, C. Tu, and D. Liu, "New control method of injection-type hybrid active power filter," *Power Electronics, IET*, vol. 4, no. 9, pp. 1051–1057, November 2011.

[13] B. Francis and W. Wonham, "Internal model principle in control theory," *Automatica*, vol. 12, pp. 457–465, 1976.

[14] M. F. Byl, S. J. Ludwick, and D. L. Trumper, "A loop shaping perspective for tuning controllers with adaptive feedforward cancellation," *Precision Engineering*, vol. 29, no. 1, pp. 27 – 40, 2005.
[15] Z. Shuai, A. Luo, C. Tu, and D. Liu, "New control method of injection-type hybrid active power filter," *IET Power Electronics*, vol. 4, pp. 1051–1057(6), November 2011.
[16] M. Steinbuch, "Repetitive control for systems with uncertain period-time," *Automatica*, vol. 38, pp. 2103–2109, 2002.
[17] W. Messner and M. Bodson, "Design of adaptive feedforward controllers using internal model equivalence," in *Proc. of the American Control Conference*, 1994, pp. 1819–1623.
[18] R. Costa-Castelló, R. Grinó, and E. Fossas, "Resonant control of a single-phase full-bridge unity power factor boost rectifier," in *IEEE International Conference on Control Applications*, 2007, pp. 599 – 604.
[19] A. Vidal, F. D. Freijedo, A. G. Yepes, J. Malvar, O. Lopeza, and J. Doval-Gandoy, "Transient response evaluation of stationary-frame resonant current controllers for grid connected applications," 2014.
[20] C. Johnson, "Accomodation of external disturbances in linear regulator and servomechanism problems," *IEEE Transactions on Automatic Control*, vol. AC-16, no. 6, pp. 635 – 644, December 1971.
[21] ——, "Real-time disturbance-observers; origin and evolution of the idea part 1: The early years," in *System Theory, 2008. SSST 2008. 40th Southeastern Symposium on*, New Orleans, USA, March 2008, pp. 88 –91.
[22] J. Han, "From PID to active disturbance rejection control," *IEEE Transactions on Industrial Electronics*, vol. 56, no. 3, pp. 900 –906, March 2009.
[23] Z. Gao, "Active disturbance rejection control: a paradigm shift in feedback control system design," in *American Control Conference, 2006*, Minneapolis, USA, June 2006, pp. 2399–2405.
[24] Z. Gao, Y. Huang, and J. Han, "An alternative paradigm for control system design," in *Proceedings of the 40th IEEE Conference on Decision and Control, 2001.*, vol. 5, Orlando, USA, 2001, pp. 4578–4585.
[25] H. Sira-Ramírez and V. Feliu-Batlle, "Robust Σ - Δ modulation-based sliding mode observers for linear systems subject to time polynomial inputs," *International Journal of Systems Science*, vol. 42, no. 4, pp. 621–631, 2011.
[26] A. Luviano-Juárez, J. Cortés-Romero, and H. Sira-Ramírez, "Synchronization of chaotic oscillators by means of GPI observers," *International Journal of Bifurcations and Chaos in Applied Science and Engineering*, vol. 20, no. 5, pp. 1509–1517, May 2010.
[27] S. Li, J. Yang, W.-H. Chen, and X. Chen, "Generalized extended state observer based control for systems with mismatched uncertainties," *IEEE Transactions on Industrial Electronics*, vol. 59, no. 12, pp. 4792–4802, December 2012, dOI: 10.1109/TIE.2011.2182011.
[28] R. Costa-Castelló, R. Griñó, R. Cardoner Parpal, and E. Fossas, "High-performance control of a single-phase shunt active filter," *IEEE Transactions on Control Systems Technology*, vol. 17, no. 6, pp. 1318–1329, Nov. 2009.
[29] R. Griñó and R. Costa-Castelló, "Digital repetitive plug-in controller for odd-harmonic periodic references and disturbances," *Automatica*, vol. 41, pp. 153–157, Sep. 2005.
[30] G. Escobar, P. G. Hernandez-Briones, P. R. Martinez, M. Hernandez-Gomez, and R. E. Torres-Olguin, "A repetitive-based controller for the compensation of $6l \pm 1$ harmonic components," *IEEE TRANSACTIONS ON INDUSTRIAL ELECTRONICS*, vol. 55, no. 8, pp. 3150–3158, 2008.
[31] J. hua She, M. Fang, Y. Ohyama, H. Hashimoto, and M. Wu, "Improving disturbance-rejection performance based on an equivalent-input-disturbance approach," *IEEE Transactions on Industrial Electronics*, vol. 55, no. 1, pp. 380–389, 2008.
[32] C.-T. Chen, *Analog and Digital Control System Design*. Saunders College Publishing, 1993.
[33] B. D. O. Anderson and J. B. Moore, *Optimal control: linear quadratic methods*. Upper Saddle River, NJ, USA: Prentice-Hall, Inc., 1990.
[34] D. E. Rivera, M. Morari, and S. Skogestad, "Internal model control: Pid controller design," *Industrial & Engineering Chemistry Process Design and Development*, vol. 25, no. 1, pp. 252–265, 1986.
[35] K. J. Astrom and T. Hagglund, *Advanced PID control*. Advanced PID control: ISA, 2006.